

Memories of migrations past: Sociality and cognition in dynamic, seasonal environments

Eliezer Gurarie^{1,2,*}, Sriya Potluri¹, G. Christopher Cosner³, R. Stephen Cantrell³, William F. Fagan¹

¹*Department of Biology, University of Maryland, College Park, MD 20742, USA.*

²*Department of Environmental and Forest Biology, SUNY College of Environmental Science and Forestry, Syracuse, NY 13210, USA.*

³*Department of Mathematics, The University of Miami, Coral Gables, FL 33146, USA.*

Correspondence*:
Eliezer Gurarie
egurarie@umd.edu

2 ABSTRACT

3 Seasonal migrations are a widespread and broadly successful strategy for animals to exploit periodic and
4 localized resources over large spatial scales. It remains an open and largely case-specific question whether
5 long-distance migrations are resilient to environmental disruptions. High levels of mobility suggest an
6 ability to shift ranges that can confer resilience. On the the other hand, a conservative, hard-wired
7 commitment to a risky behavior can be costly if conditions change.

8 Mechanisms that contribute to migration include identification and responsiveness to resources, sociality,
9 and cognitive processes spatial memory and learning. Our goal was to explore the extent to which
10 these factors interact not only to maintain a migratory behavior but also to provide resilience against
11 environmental changes. We develop a relatively simple diffusion-advection model of animal movement in
12 which an endogenous migratory behavior is modified by recent experiences via a memory process, and
13 animals have a social swarming-like behavior over a range of spatial scales.

14 We found that this relatively simple framework was able to adapt to a stable, seasonal resource dynamic
15 under a fairly broad range of parameter values. Furthermore, the model was able to acquire an adaptive
16 migration behavior with time. However, the resilience of the process depended on all the parameters
17 under consideration, with many complex trade-offs. For example, the spatial scale of sociality needed
18 to be large enough to capture changes in the resource, but not so large that the acquired collective
19 information was overly diluted. A long-term reference memory was important for hedging against a highly
20 stochastic process, but a higher weighting of more recent memory was needed for adapting to directional
21 changes in resource phenology.

22 Our model provides a general and versatile framework for exploring the interaction of memory, movement,
23 social and resource dynamics, even as environmental conditions globally are undergoing rapid change.

24 **Keywords:** Sociality, seasonal migration, collective knowledge, diffusion-advection models, spatial memory

1 INTRODUCTION

Seasonal migrations are widespread among terrestrial, aquatic, avian and invertebrate species (Dingle, 2014). For many species, migration is an extremely successful strategy, allowing a far greater number of individuals to inhabit landscapes which might not otherwise be able to support large numbers year round (Fryxell et al., 1988). The evolutionary stability of a migratory strategy essentially relies on the fitness benefits of accessing seasonal resources, whether for energetic gain, predator avoidance, or a suitable environment for reproduction, outweighing the energetic and survival related costs of migration (Avgar et al., 2014).

Proximate causes, drivers and mechanisms for migration vary widely across and even within species (Berthold, 1999; Shaw, 2016). Some migrants follow a “green wave” of spring vegetation as it flowers across altitudinal or latitudinal gradients (Bischof et al., 2012; Kölzsch et al., 2015; Merkle et al., 2016). These migrations can be considered “tactical”, as they can occur - as an extreme simplification - purely as response to local conditions. Other migrants perform long-distance migrations in anticipation that critical resources will be available at the time of arrival at the end point of migration (Abrahms et al., 2019). This second behavior involves the greatest trade-off between the costs and benefits of accessing those highly seasonal and localized resources. This approach can be considered “strategic” in the sense that it is driven not by immediate cues but by an anticipation based on prior experience (Bracis and Mueller, 2017; Merkle et al., 2019; Bauer et al., 2020).

While migration can be a very successful strategy, with migratory ecotypes of the same species often outnumbering non-migratory conspecifics. Migratory caribou and reindeer *Rangifer tarandus*, for example, are several orders of magnitude more abundant than non-migratory woodland, mountain and forest ecotypes (Festa-Bianchet et al., 2011; Uboni et al., 2016). However, the question of whether migratory animals are more or less resilient to environmental disruptions in the environment remains open and largely case-specific (Moore and Huntington, 2008; Hardesty-Moore et al., 2018; Xu et al., 2021). On the one hand, migratory species may be more vulnerable as disruptions in either of the seasonal ranges or along a migratory corridor can have significant negative impacts (Wilcove and Wikelski, 2008; Seebacher and Post, 2015; Kauffman et al., 2021). On the other hand, migratory species might be more resilient due to their general wide-ranging mobility (Robinson et al., 2009). The resilience of a migratory populations depends on the plasticity and adaptability of a population, which can take multiple forms, reflecting variation in *where*, *when* and *whether* the migration occurs (Gurarie et al., 2017; Xu et al., 2021).

Cognitive processes, in particular spatial memory, have been shown to be important mechanisms for the reinforcement and maintenance of migration (Merkle et al., 2019; Bauer et al., 2020). Similarly, sociality and social learning are likely essential to maintaining migration (Guttal and Couzin, 2010; Fagan et al., 2011; Jesmer et al., 2018; Berdahl et al., 2018). However, the interacting role of sociality and spatial memory for the plasticity of migration and the resilience of the behavior when faced with a changing environment are generally unknown, though it has been hypothesized that the importance of these cognitive processes depend on the predictability of these resources (Riotte-Lambert and Matthiopoulos, 2020). Because the scenarios underlying migration are manifold and complex, mathematical modeling may provide some insights and help clarify where, when, and under what conditions we might expect migration behavior to emerge, to be adaptive, to be maladaptive, or to collapse.

Here, we develop a diffusion-advection model with sociality and memory to explore the resilience of a migratory population under various dynamic, seasonal resource distributions. In formulating the model, our goal was to identify the minimum set of movement and memory parameters required to generate an adaptive, migratory behavior. This includes the ability to learn to migrate from non-migratory initial conditions, simulating the release of naive animals in a seasonal environment (Jesmer et al., 2018), to lose the propensity to migrate if the resource distribution does not require it, also a commonly observed phenomenon (Wilcove and Wikelski, 2008), and to assess the resilience or fragility of a migratory population against changing resource distribution dynamics, including both stochasticity and trends in spatial and temporal distributions, mirroring the effects of climate change (Park et al., 2020).

We anticipated that under many conditions a blending of *tactical* (i.e. direct response to resource availability or perception) and *strategic* (i.e. memory-driven and forward-thinking) behavior will help foragers navigate dynamic, seasonal environments. Over-reliance on either strategy should be maladaptive. We further anticipate that a shorter-term memory updating is needed to navigate trends in resource spatial distribution and temporal distribution (phenology), but that a longer-term reference memory is needed to navigate resource distributions that are stochastic (Lin et al., 2021). Similarly, we anticipated that a balance between very low sociality and extreme sociality would lead to the most resilient migratory process.

METHODS

85

2.1 Memory movement model

In designing our study, our goal was to develop a minimal heuristic in which the following processes were explicitly modeled: (1) Random or exploratory movement, (2) attraction to resources, (3) sociality in the movements, (4) a long-term (or *reference*) memory of large-scale movement behavior, and (5) a short-term (or *working*) memory that updates movement behavior based on recent experience.

A diffusion-advection equation provided a computationally efficient and versatile framework for examining just such a system. We consider a population moving in one dimension in a constrained domain D and distributing itself according to the following equation:

$$-\frac{\partial u}{\partial t} = -\varepsilon \frac{\partial^2 u}{\partial x^2} + \alpha \frac{\partial}{\partial x} \left(u \frac{\partial h}{\partial x} \right) + \beta \frac{\partial}{\partial x} (v_s(u)) + \frac{\partial}{\partial x} (u v_m(t)) \quad (1)$$

where u represents the population distributed in time and space. The first term is the diffusion term, capturing the fast time-scale exploration and “random” movements of individuals, with ε is the diffusion rate.

The second term represents the attraction to a dynamic resource h , with the proportionality of the advection to the gradient of the resource given by the parameter α (note, the population and resource distributions are functions of both space and time $u(x, t)$ and $h(x, t)$ - we omit the dependent variables in the notation for brevity). This is the well-studied standard chemotactic resource-following behavior. We borrow the general notation from earlier related work expanding diffusion-advection models to incorporate non-local information (Fagan et al., 2017) and behavioral switching (Fagan et al., 2019).

The third term captures the collective or social advection term of the population via a non-local, density dependent function $v_s(u, x)$. If this function takes the form of a convolution around a non-local kernel k , i.e. $v_s(u) = k(x) * u(x)$, and if that kernel is odd, an attractive or “swarming” behavior can be generated (Mogilner and Edelstein-Keshet, 1999). We use the kernel analyzed by Mogilner and Edelstein-Keshet (1999):

$$k(x) = \frac{x}{2\lambda^2} \exp(-x^2/2\lambda^2).$$

The convolution of u with this kernel has the property of pushing the population in a positive direction when $x < \langle u \rangle$, and in a negative direction when $x > \langle u \rangle$, where $\langle u \rangle$ is the mean location of the population. The parameter λ is a length scale of sociality, roughly one-half the size of the swarm, and β is a parameter that quantifies the overall strength of sociality.

Finally, the last term captures the direct advection that emerges from a memory-driven migratory behavior. This term evolves with a set of parameters θ_y that slowly change each year $y \in \{0, 1, 2, \dots\}$, i.e. the count of periods τ : $y = \lfloor t/\tau \rfloor$. The migration is specified by six parameters θ : the timing of the start and duration of two anticipated seasons (e.g. summer and winter) $t_1, \Delta t_1, t_2, \Delta t_2$, and the spatial coordinates of the population centroid for each season x_1 and x_2 . The remembered migratory speed term is a simple step function given by:

$$v_m(t, \theta_y) = \begin{cases} 0; & t > t_1 \text{ and } t \leq t_1 + \Delta t_1 \\ s_{12}; & t > t_1 + \Delta t_1 \text{ and } t \leq t_2 \\ 0; & t > t_2 \text{ and } t \leq t_2 + \Delta t_2 \\ s_{21}; & t > t_2 + \Delta t_2 \text{ or } t \leq t_1 \end{cases} \quad (2)$$

where the migration speeds s_{12} and s_{21} from the respective ranges are set such that they arrive at x_1 at t_1 , depart at $t = t_1 + \Delta t_1$, arrive at x_2 at $t = t_2$, and depart at $t_2 + \Delta t_2$. Thus, $s_{12} = (x_2 - x_1)/(t_2 - (t_1 + \Delta t_1))$ and $s_{21} = (x_1 - x_2)/(t_1 - (t_2 - \tau + \Delta t_2))$. This step-like migration function is a one-dimensional version of the migration parameters estimated for individuals (Gurarie et al., 2017) and populations (Gurarie et al., 2019) in empirical studies.

We consider these six parameters to be the known or remembered determinants of the migratory behavior, with an initial set θ_0 determining the reference migration behavior. This reference migration is updated each year by the experience of the population. To perform this updating, we estimate a new set of parameters $\widehat{\theta}_y$ after each year, and combine these new parameters with the reference parameters according to the following weighted mean:

$$\theta_{y+1} = \kappa^y \theta_o + (1 - \kappa^y) \widehat{\theta}_y \quad (3)$$

where each of the six parameters is updated according to equation 3 identically. The estimates $\widehat{\theta}_y$ are obtained via a least-squares minimization of the migration track ($m(t, \theta) = \int_0^t v_m(t', \theta_y) dt'$) against the spatial mean of the population process in year y (i.e. $\widehat{u}(t) = \int_X u_y(t, x) dx$). The parameter $\kappa \in (0, 1)$ captures the reliance on that long-term memory. When $\kappa = 0$, all of the actionable memory is from the preceding year. When $\kappa = 1$, the actionable memory is entirely the reference memory.

The model is confined to a one-dimensional bounded domain $[-\chi, \chi]$, with no flux outside of the boundaries. Formally, this no-flux condition means the following conditions must be met

$$\begin{cases} \varepsilon \frac{\partial u}{\partial x} - \alpha \left(u \frac{\partial h}{\partial x} \right) - \beta(v_x(u)) - (uv_m(t)) = 0 & \text{where } x = \chi \\ -\varepsilon \frac{\partial u}{\partial x} - \alpha \left(u \frac{\partial h}{\partial x} \right) - \beta(v_x(u)) - (uv_m(t)) = 0 & \text{where } x = -\chi \end{cases}$$

In practice, the design of our resource space (see below) and other parameterization lead 0 or near 0 values of both $h(x)$ and $u(x)$, and the simpler $\partial u(-\chi, t)/\partial t = \partial u(\chi, t)/\partial t = 0$ boundary condition provides a good approximation.

As there are no birth or death processes, the total population remains fixed and constant, for convenience integrating to 1. Furthermore, the parameters remain constant throughout time, with no adaptation or mutation-selection process. Our interest is in the ability of a fixed set of movement and memory parameters to navigate an intra- and interannually dynamic, seasonal environment.

2.2 Seasonal resource

We ran this model on a spatial domain $x \in [-100, 100]$, and a periodicity $\tau = 100$ (i.e. 100 day years). We were interested in an approximately periodic resource dynamic, i.e. one in which $h(x, t) \approx h(x, t - \tau)$. We generated two types of resource distributions. A “non-survable” resource (*island resource*), and weakly survable resource (*drifting resource*). Both are characterized by a peak in time and space centered at m_x at m_t , and $-m_x$ at $\tau - m_t$ (for example, locations 30 and -30 at times 25 and 75, respectively). These pulses have a shared time scale of duration s_t and a spatial scale of extent s_x , the standard deviation in the time and space dimension respectively. The island resource is simply two uncorrelated bivariate normal distributions

$$h(x, t) = K (\Phi(m_x, m_t, s_x, s_t) + \Phi(-m_x, \tau - m_t, s_x, s_t))$$

where Φ is the bivariate Gaussian distribution function, and the normalizing constant K is selected such that the average total amount of resource throughout the year is 1, i.e. $\frac{1}{\tau} \int_T \int_X h(x, t) dx dt = 1$.

The drifting resource differs from the island resource in that the total amount of resource at any given time $\int_X h(x, t) dx = 1$. This property is attained by distributing the resource as a re-scaled beta distribution, where the shape and scale parameters vary sinusoidally in such a way as to make the standard deviations and means match the desired values of m_x, m_t, s_x, s_t (see Supplementary Materials for details). Both types of resources are illustrated in figure 1.

Within a given year, the resource is entirely symmetric: $h_y(x, t) = h_y(-x, \tau - t)$. However, in scenarios exploring climate change we allow the peaks to vary with directional trend and stochasticity according to: $m_x(y) \sim N(\mu_x + \gamma_x y, \sigma_x)$ and $m_t(y) \sim N(\mu_t + \gamma_t y, \sigma_t)$, where the μ , γ and σ terms are the mean, slope and variance, respectively, for the location and time duration of the pulse. Thus, if $\gamma = 0$ and $\sigma = 0$, the conditions are constant across years and if $\gamma_x > 0$ there is a shift of the resource towards the extremes of the domain. While we did not explore phenological shifts in timing, those can readily be modeled as well. These trends model the pole-ward shift of peak resources and the earlier spring phenology occurring with a warming global climate (Renner and Zohner, 2018). The spatial and temporal scales of the resource peak (s_x and s_t) remain constant in all of our simulations.

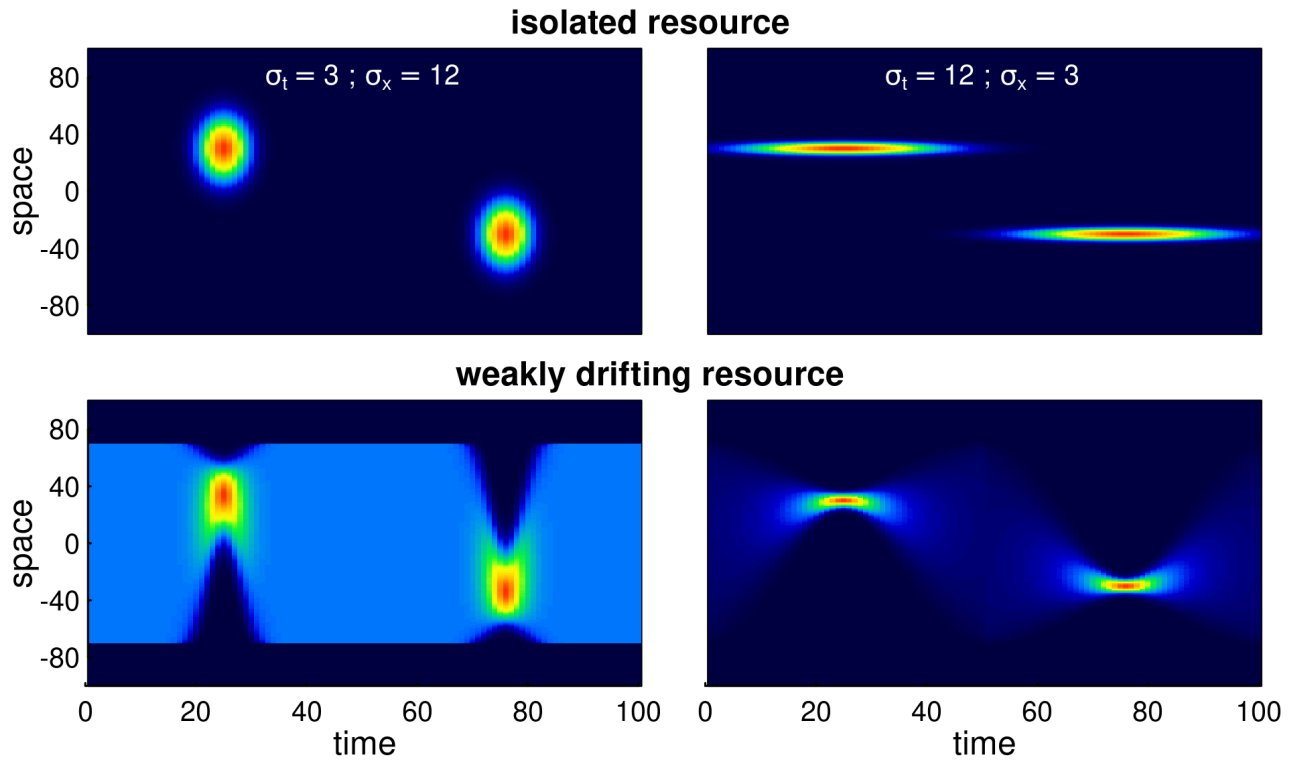


Figure 1. Examples of various seasonal resource distribution functions, contrasting short duration, but wide pulses ($\sigma_t = 3, \sigma_x = 12$; left panels), long duration but spatially concentrated pulses ($\sigma_t = 12, \sigma_x = 3$; right panels), and isolated resource pulses (upper panels) from the weakly drifting resource (lower panels). The total amount of resource is identical across all scenarios. In the weakly drifting resources, the total amount is constant at all times, and uniform in the middle of the phase (time = 0, 50, 100).

2.3 Metrics

The main metrics we were interested in are *migration mismatch*, *foraging efficiency* and *adaptation to directional trends*.

Migration mismatch captures the combined difference between the migration phenology and the resource phenology in time and space. Spatial mismatch MM_x is the absolute difference between the migration targets and the resource peaks: $MM_x = |x_1 - m_x| + |x_2 + m_x|$. Temporal mismatch is the difference between the arrival time and the peak of the resource if arrival is post-peak, the difference between the departure time and the peak of the resource if departure is pre-peak, and 0 if the seasonal duration spans the peak, i.e. $MM_t = \max\{t_1 - m_1, m_1 - (t_1 + \Delta t_1), 0\} + \max\{t_2 - m_2, m_2 - (t_2 + \Delta t_2), 0\}$. Thus, the total mismatch is the sum of these: $TM = MM_x + MM_t$. A mismatch of less than 1 is essentially perfect, a mismatch of 1-5 we consider excellent, and beyond 50 the system can be said to have failed to keep track of the resource dynamics.

To quantify the foraging efficiency, i.e. the organisms' ability to track the distribution of the resources over space and time, we use a continuous form of the Bhattacharyya coefficient (Bhattacharyya, 1943) which quantifies the similarity between two distributions. We compute this coefficient at every time point in a given year, and take the mean across the equilibrium year to determine foraging efficiency (FE). Thus, the foraging efficiency index is:

$$FE = \frac{1}{\tau} \int_0^{\tau} \int_{-\chi}^{\chi} \sqrt{u(x, t) h(x, t)} dx dt$$

where the spatial integral is taken over the domain. This metric is constrained to be between 0 and 1.

For simulations with a constant resource, we ran the model until a quasi-equilibrium (stationary) state was achieved, i.e. where the Bhattacharya index of the population distribution across subsequent years reached a value of 0.99999. Once stationarity was attained, we computed the migration mismatch and foraging efficiency metrics, as well as the number of years required to reach stationarity.

For numerical runs with climate change, we first run a simulation with a given parameter set until stationarity, as above, and then begin shifting the location of the resource poleward with a slow, moderate or rapid trend ($\gamma_x = 0.25, 0.5$ and 1 , respectively), and / or by adding stochasticity (spatial standard deviation 3, 6, 9 or 12). For stochasticity analyses, we compare foraging efficiency across a range of the reference memory parameter κ . For analyses that included directional trends, with or without stochasticity, we quantified the ability of the system to keep track of climate change with a *spatial adaptation* (SA) index. This index is the ratio of the slope of the memory-based migration location over time, i.e. $SA = \hat{\gamma} / \gamma_x$ where the adaptation slope estimate is the regression coefficient of the spatial coordinate of the migration against time (i.e. $m_{x,i} = \hat{\gamma}_x i + m_{x,0}$, where i is the year), and γ_x is the rate of drift of the resource peak (table 1). An SA equal to 1 suggests that the process is keeping up with climate change, an SA of 0 indicates that the process is not responding at all to climate change. Values greater than 1 (super-adaptation) are possible, as are values less than 1, which correspond to a loss of migration behavior.

All movement model parameters, resource parameters, and metrics are summarized in table 1.

2.4 Simulation studies

We explored this model using numerical differencing of a system of ordinary differential equations (ODE's) approximating the PDE in equation 1 with the Runge-Kutte algorithm using the `deSolve` (Soetaert et al., 2010) and `ReacTran` (Soetaert and Meysman, 2012) packages in R. We additionally used the `nlsLM` function in package `minpack.LM` (Elzhov et al., 2016) for robust and fast annual estimation of the migration parameters. The complete code is available as an R package (`memorymigration`) available on GitHub at <https://github.com/EliGurarie/memorymigration> and as an interactive Shiny application at <https://spot3512.shinyapps.io/memorymigrationshinyapp/>.

We assessed a wide range of parameter values and resource geometries and dynamics with the goal of answering the four main questions: (1) Can this model adapt to a discrete shift in peak resource location and timing? What is the relative role of memory and sociality for adaptation? (2) Can this model acquire a migratory behavior from a non-migratory initial condition? (3) What is the role of a reference memory for dealing with stochastic resource dynamics? (4) Can this model adapt when the resource peaks shifts in space? Details of parameter combinations and reported metrics are provided in respective results sections.

3 RESULTS

3.1 Adaptation to resource phenology

The ability of this system to attain a stable, migratory state that matches the dynamics of the resource is illustrated in figure 2. In the illustrated scenario, it takes nearly 40 years to attain an equilibrium, and the eventual steady state is one where the centroid of the migration lines up exactly with the centroid of the resource, and the arrival timing coincides with the *peak* of resource availability. Notably, the path to this equilibrium is somewhat indirect, with the later winter range taking more time to stabilize than the earlier summer range. The eventual steady state is one where the foraging efficiency is relatively high, near 0.6 compared to an initial value of 0.3. However, the increase in the foraging efficiency was not entirely monotonic, as the system moved through some slightly sub-optimal stages in adjusting its migration behavior.

We ran this process for 8100 parameter combinations crossing different values of the movement process (α , β and λ) and resource characteristics (σ_x and σ_t), and present the total mismatch (TM) against all those combinations in figure 3. In all of these simulations, memory was entirely recent ($\kappa = 0$), since there can be no benefit to relying on a sub-optimal reference memory. We compared a set of diffusion rates ε between 1 and 8, but only illustrate results for $\varepsilon = 4$.

A well-matched migration phenology ($TM < 5$) occurred under very many combinations of parameter values, but all parameters play interacting roles. Among the more intuitive results are that greater values of α (resource following) lead to an improved ability to match the migration. Resource peaks with larger spatial extent (higher σ_x) are generally better for migration matching.

Less intuitive was the high importance of the sociality parameters, in particular the spatial scale of the swarming. Higher levels of social attraction (β) led to improved migration matching except

Table 1. Table of parameters, variables and metrics.

Memory migration model	
ε	Diffusion
α	Strength of resource following
β	Strength of sociality
λ	Spatial scale of sociality
κ	Proportion of reference versus working memory
x_1, x_2	location of population centroids in summer and winter
$t_1, \Delta t_1$	start and duration of summer season
$t_2, \Delta t_2$	start and duration of winter season
κ	proportion memory allocated to reference (long-term) memory vs. working (short-term) memory
Resource dynamics	
τ	duration of period (year)
$m_x, -m_x$	spatial coordinate of resource peak for summer and winter
$m_t, \tau - m_t$	timing of resource peak for the summer and winter
σ_x, σ_t	time duration and and spatial scale of resource pulse
γ_x, γ_t	rate of change of peak location and timing of resource
ψ_x, ψ_t	standard deviation of peak location and timing
Metrics	
MM_x	spatial migration mismatch
MM_t	temporal migration mismatch
TM	total mismatch
FE	foraging efficiency
SA	spatial adaptation index

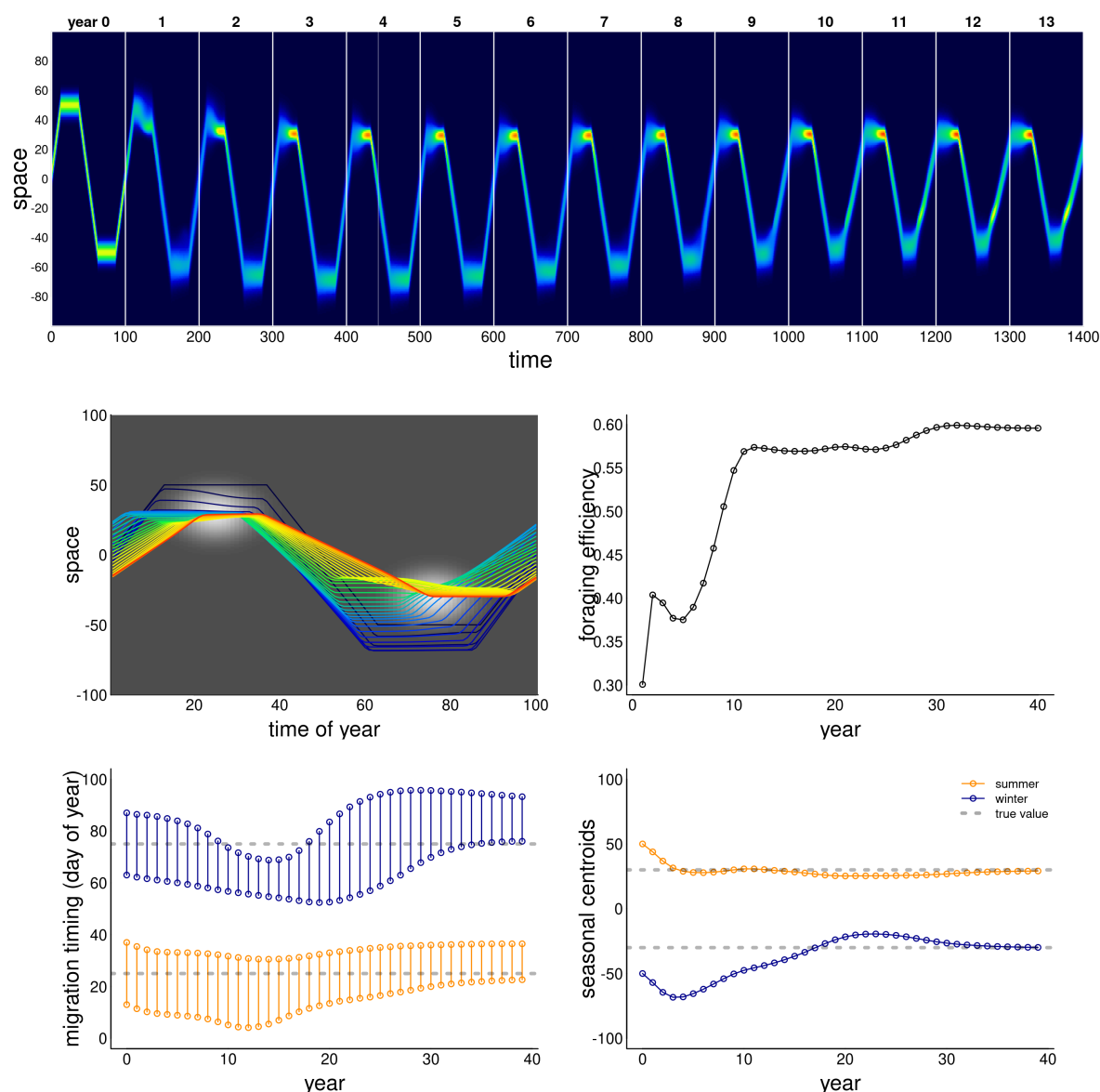


Figure 2. Example of adaptation to a shift in resource peak. The initial (year 0) behavior migrates to locations 50 and -50 at days 15 and 60, whereas the resource peak is at 30 and -30, peaking at times 25 and 75. The panels show (a) the first 14 years of the simulation; (b) the centroid of the annual movement of the population is shown in panel b, with dark blue to red colors indicating year 0 to year 40; (c) annual foraging efficiency across years; (d) migration timing parameters for each year, with orange segments indicating arrival and departure from the summering (northern) grounds, and the blue segments indicating timing of arrival and departure at the wintering grounds; (e) migration arrival and departure location across years, with blue and orange indicating winter (southern) and summer (northern) locations.

in those cases where the sociality scale λ was high. Thus, for example, at $\lambda = 20$, no simulations at $\beta \geq 200$ managed to acquire or maintain a matched migration. However, at $\lambda = 50$ or 100, the migration was slightly better matched at high values of β (figure 3). The spatial extent of the swarm was a remarkably significant variable. Smaller swarms were able to match migration only at low values of social attraction ($\beta = 200$), and relatively high values of resource attraction ($\alpha \geq 600$).

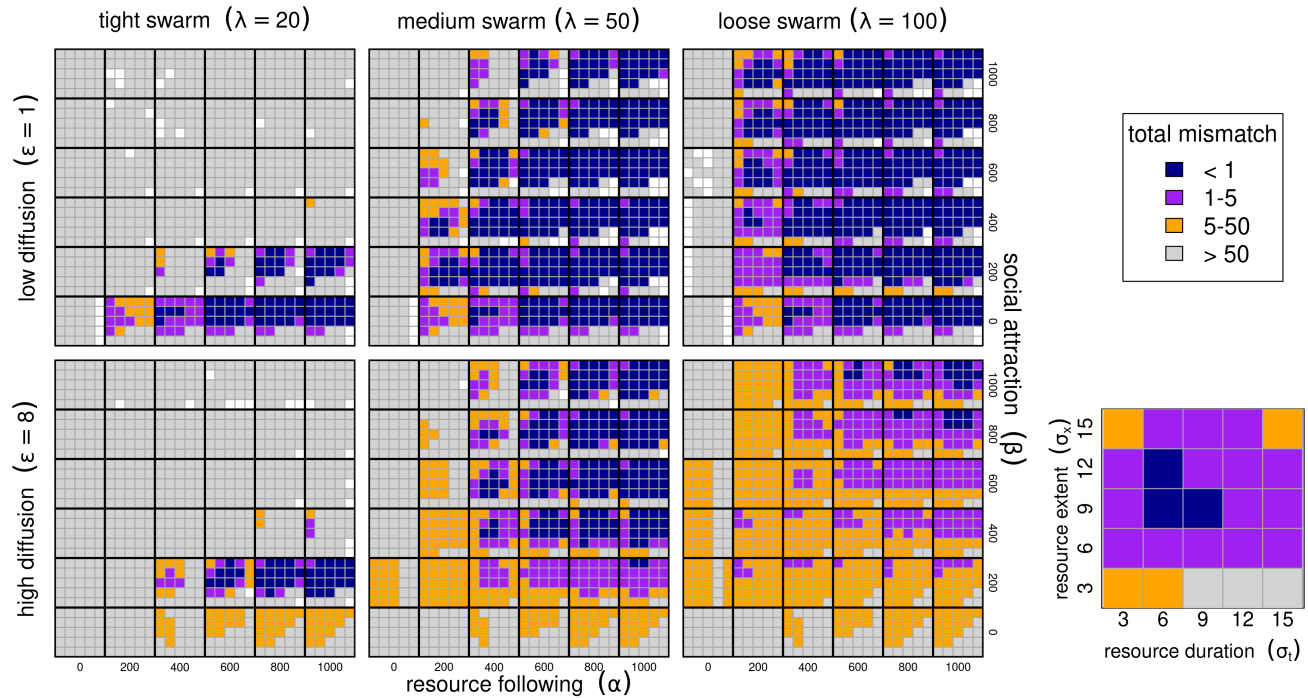


Figure 3. Migration phenology matching across six model parameters. Low and high diffusion ($\varepsilon = 1$ and 8 in upper and lower panel blocks), tight, medium and loose swarms ($\lambda = 20, 50, 100$) left to right panels. Within each of these blocks, high values of the resource following parameters α from 0 to 1000 are left to right, and higher values of the sociality parameter β are bottom to top. Within each of the combinations of $\varepsilon, \lambda, \alpha, \beta$, we show results ranging across 6 values of resource duration (σ_t , 3 to 15 left to right), and 6 values of resource extent (σ_x , 3 to 15 bottom to top), as in the zoomed-in panel (bottom right; drawn from $\alpha = 200, \beta = 200, \lambda = 100$). The color scheme reflects the total mismatch, i.e. the sum of the absolute differences between the migration timing and locations from the resource peak.

250 Random forest analyses, whether on the log of total mismatch or on the classification of a perfect
 251 match, uniformly show that the most important variables (Breiman, 2001) were α and λ (4.14 and
 252 4.02 proportional increase in MSE), and the least important was σ_t , with a 0.5 proportional increase.

253 Overall, foraging efficiency was strongly correlated with migration matching, as expected. At high
 254 mismatch (> 50), foraging efficiency was low (mean 0.29, s.d. 0.16) compared to the near-perfect
 255 matching migrations (mean 0.58, s.d. 0.14). However, somewhat higher mismatch (1 to 5) showed
 256 an even higher overall foraging efficiency (mean 0.62, s.d. 0.18 - see also figure 4).

257 3.2 Learning to migrate

258 Figure 5 illustrates the ability of the model animals to learn to migrate in a weakly drifting
 259 resource environment with a narrow pulse of resource peaking at 30 and -30 (at days 25 and 75), but
 260 a uniform distribution of resource at times 0 and 50 . In order to learn to migrate, the system needed
 261 to have a higher exploratory impulse (higher diffusion constant ε), a stronger resource advection
 262 (higher α) and somewhat weaker sociality (lower β). The qualitative behavior of this process was
 263 to start drifting towards the summer resource, while slowly developing a weak pulse towards the
 264 winter resource as well. After first locking in on the summer resource, the winter migration, driven
 265 both by high diffusion and high resource following, slowly extended itself until both narrow peaks of
 266 resource were consistently reached.

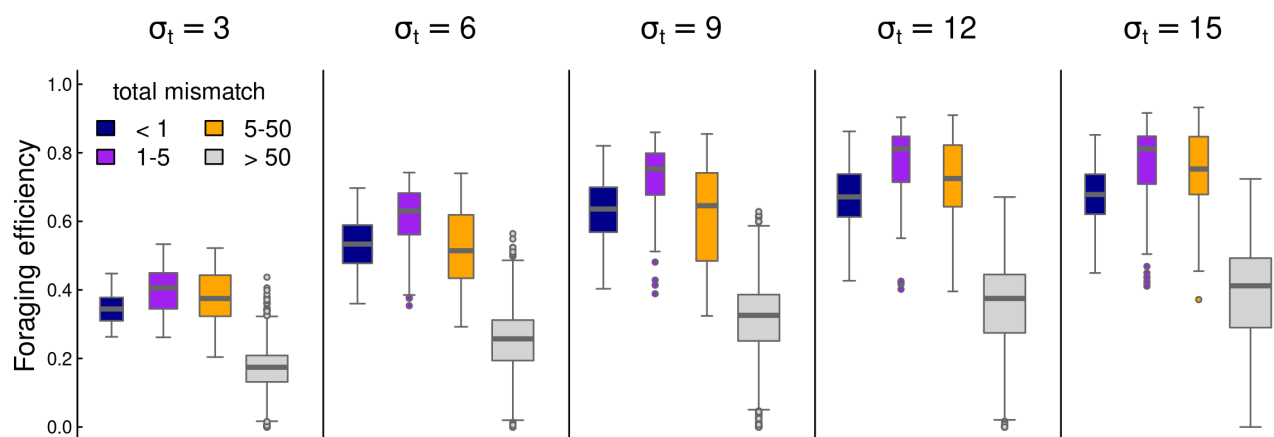


Figure 4. Box-plots of foraging efficiency against mismatch across several values of foraging patch duration.

267 The model had, in general, a difficult time learning migration from a non-migratory initial condition.
 268 Out of 4047 successful runs, only 4 attained mismatch below 1, and 130 below 5. Conditions that
 269 were more conducive to learning migration were pulses of *longer* duration (high σ_t), but *smaller*
 270 in scope (low σ_x), suggesting that the feedback that encourages migration needs to be compact in
 271 space but long enough in duration to lock in to the memory.

272 3.3 Directional climate change

273 To assess the ability of the system to adapt to a trending climate, we generated scenarios with
 274 slow, moderate and fast outward directional shifts in the resource peak (0.25, 0.5 and 1 units / year,
 275 respectively). We then assessed 40 parameter combinations for each of those scenarios, high and
 276 low values of resource following ($\alpha = 400$ and 100), high and low values of sociality ($\beta = 400$ and
 277 100) and 10 values of the spatial scale of sociality ($\lambda = 20$ to 200). The spatial and temporal scale
 278 of the resource pulses were fixed to $\sigma_x = 12$ and $\sigma_t = 6$, a combination which analyses in section
 279 3.1 showed were generally “easy” to adapt to. We computed the adaptation index and foraging
 280 efficiency for each of the 120 runs (figure 6). We were interested in the dynamics against λ due to
 281 the consistently high importance of this parameter for matching migration in steady states. Our
 282 main index of interest was the spatial adaptation (SA) to trends.

283 As figure 6 shows, higher values of resource following ($\alpha = 400$; orange circles) are nearly universally
 284 better for keeping up with climate change (SA values near 1). Furthermore, when combined with
 285 high sociality ($\beta = 400$; right panels), nearly all parameter combinations do a good job keeping up
 286 with climate change (SA values ranging between 0.53 and 0.85 for a swarm size greater than 50).
 287 However, that maximum value is still less than 1, suggesting that truly matching a steadily drifting
 288 trend is very difficult. Smaller social spatial scales ($\lambda < 50$) have a very hard time adapting when
 289 the social attraction is high, but do fairly well when social attraction is low. Larger sized swarms do
 290 progressively worse across more parameterizations, e.g. in the most rapid climate change scenario,
 291 the SA drops from 0.83 to -0.13 as the swarm increases in size from 40 to 200 (encompassing,
 292 essentially, the entire spatial domain).

293 A rather more dramatic pattern is visible for the lower foraging attraction scenario ($\alpha = 100$; blue
 294 circles). Notably, no parameter combination at this value comes close to keeping up with the rapid

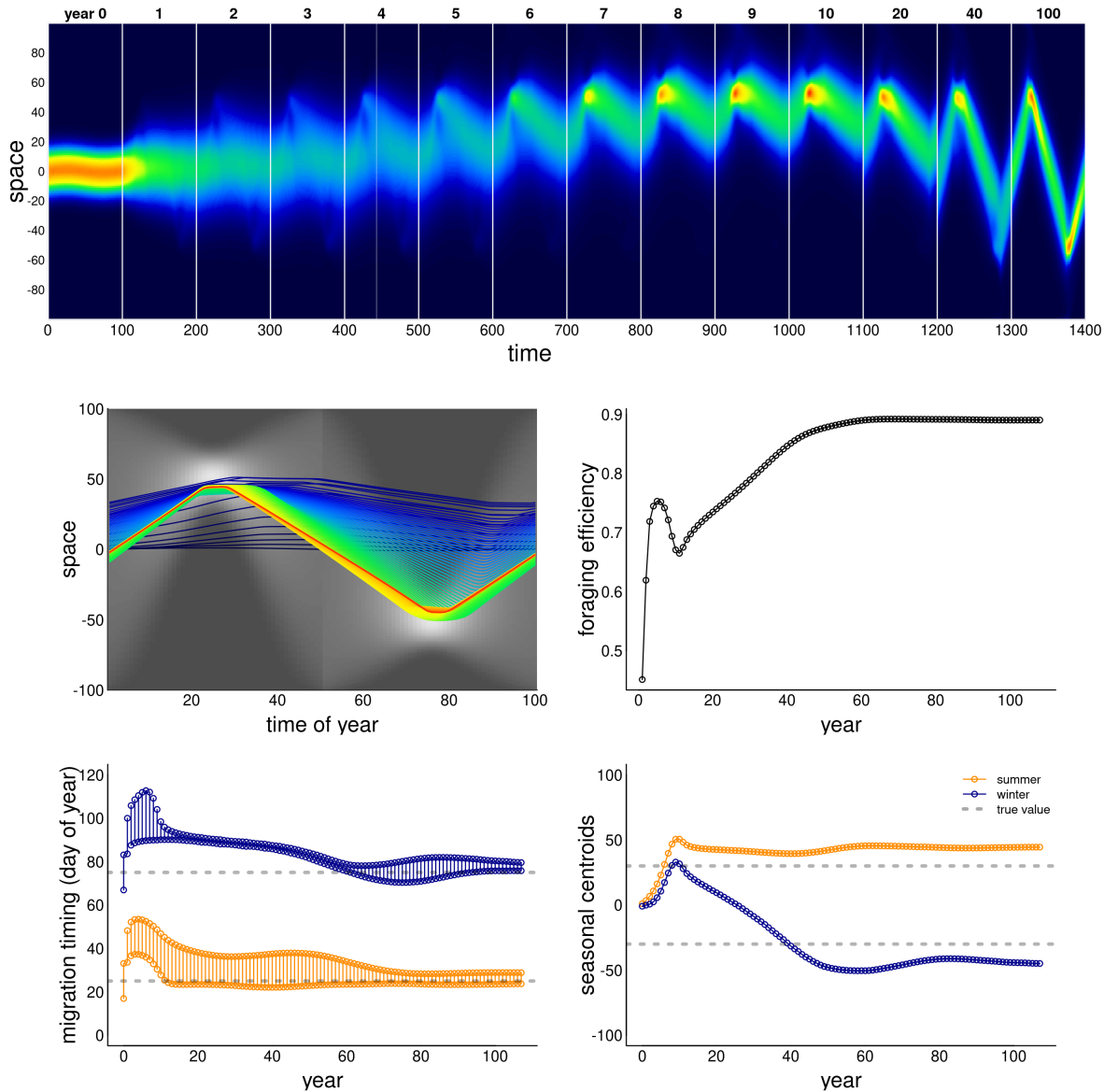


Figure 5. Example of model learning to migrate. The resource is a “weakly drifting” resource and the initial (year 0) condition is non-migratory. The simulation was run for 100 years, and a sampling of those years (labeled) are presented in panel a: all years from 0 to 10, followed by 20, 40 and 100. Otherwise, panels are as in figure 2. Additional parameter values were $\varepsilon = 5$, $\alpha = 500$, $\beta = 50$ and $\lambda = 40$.

295 climate change (SA range -0.64 to 0.13). For slower climate change, however, there is a window of
 296 values for the swarm size between 40 and 80, where the SA *exceeds* 1, but then crashes quite rapidly
 297 to negative values of SA as that swarm size increases. These “super-adaptive” processes indicate a
 298 unique sweet spot where a swarm is large enough to capture and adapt to the drifting resource,
 299 but not so large that the information gathered in a given year is too weak to adjust the migratory
 300 behavior in a following year.

301 As anticipated, better adaptation to the drifting resource correlated strongly with higher foraging
 302 efficiency (inset boxplots).

303

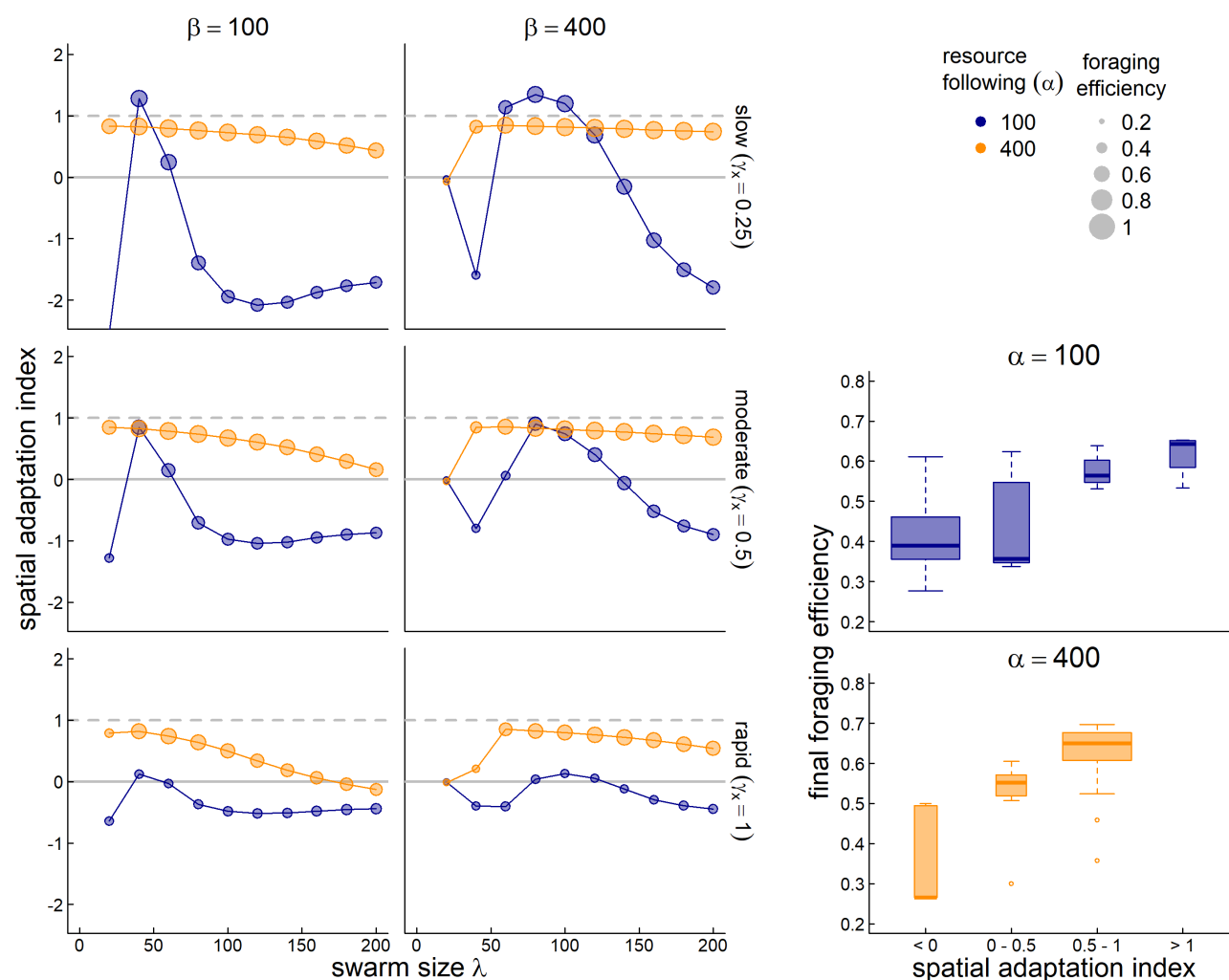


Figure 6. Adaptation to a steadily drifting resource. In three scenarios, the spatial coordinates of the resource drift by 0.25, 0.5, and 1 unit per year (top to bottom, respectively). The y-axis is the spatial adaptation index (SA), i.e. the trend of the memory-driven migration divided by the resource drift trend. Values near 1 indicate a behavior that keeps up with climate change, values near 0 indicate no change in migration behavior, and negative values indicate a trend that is opposite to the climate trend. We compare across spatial scales of sociality (λ - x-axis), for low and high values resource following ($\alpha = 400$ and 100 - orange and blue dots) and low and high values of sociality ($\beta = 100$ and 400 , left and right panels). The size of the circles is proportional to the foraging efficiency of the resulting parameter combinations. The bottom-right boxplots indicate the final year foraging efficiency against SA; purple and blue boxes indicate the highest values, orange and gray lower values.

3.4 Reference memory and stochasticity

While recent memory can be helpful for adapting to a single novelty or a smoothly changing conditions, we hypothesized that more conservative approach that relies on a reference memory may be beneficial when conditions change stochastically. We tested this hypothesis by solving a set of models across a range of κ values from 0 (all recent memory) to 1 (all reference memory). In these scenarios, we ran the system for as many years as needed with no stochasticity to acquire a stationary state (i.e. similarity index greater than $1-1e-6$). We then used the stationary state

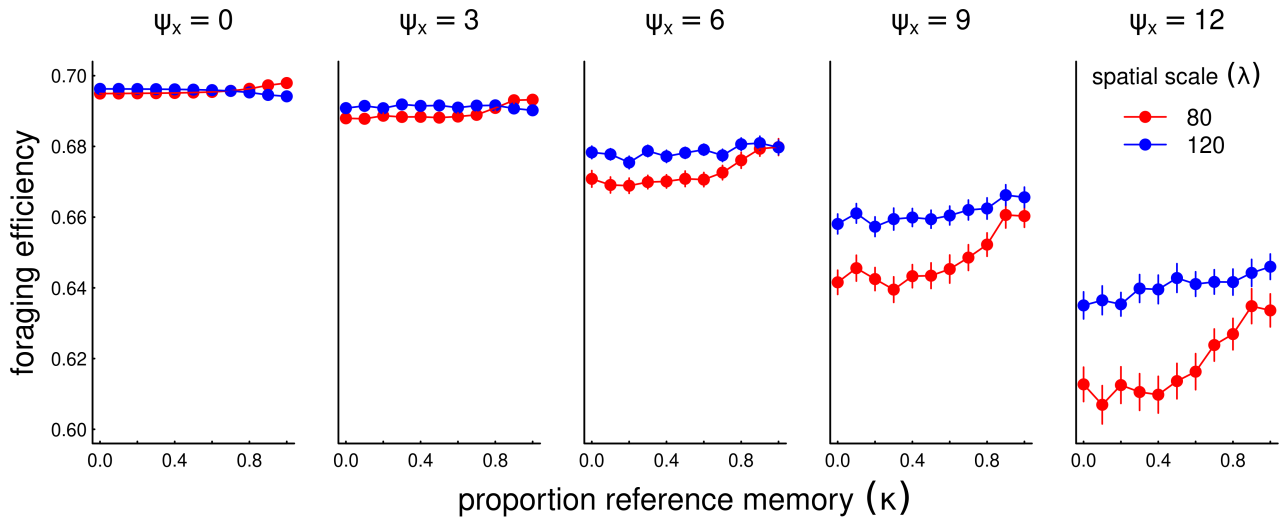


Figure 7. Foraging efficiency (FE) across various values of reference memory κ (x-axis) for increasing amounts of interannual stochasticity (ψ_x , panels left to right), and two values of sociality spatial scale $\lambda = 80$ and 120. For the processes with non-zero stochasticity ($\psi_x > 0$), the process was run 90 times for values of κ . Points represent the average of the FE's across all 50 years and 90 replicates, and shaded areas represent a local regression (loess) smooth of FE against κ . In these scenarios, the resource following parameter $\alpha = 100$, the social attraction $\beta = 400$ and diffusion $\varepsilon = 4$.

311 as the reference memory, and then ran the process for an additional 50 years with a stochasticity
 312 (i.e. standard deviation in peak location of the resource) ranging from 0 to 12, and present the
 313 resulting average foraging efficiency (figure 7).

314 Overall, as expected, the greater the stochasticity, the lower the foraging efficiency. Further, as we
 315 predicted, highest level of κ can significantly help foraging efficiency, with some variation across the
 316 spatial scale of sociality, especially in more highly stochastic scenarios. When that scale of sociality is
 317 high enough ($\lambda = 120$, blue colors) there is greater probability of overlap with a stochastic resource,
 318 and a conservative, stable migratory regime is much more beneficial in the long run.

319 3.5 Stochasticity and trends

320 We added 30 years of directional trends to the variously stochastic process described above, and
 321 assessed the adaptation index against the reference memory parameter κ (figure 8). Over-reliance on
 322 reference memory ($\kappa = 1$) by definition does not allow the system to keep up with climate change,
 323 leading to an adaptation index of 0. However, in many cases a balancing of recent and reference
 324 memory (κ value between 0.6 and 0.8) in many cases was slightly but significantly better than
 325 relying entirely on recent memory. The smaller spatial scale (in the selected parameter space) does a
 326 generally better job than the larger spatial scale at lower stochasticity. At higher level of stochasticity,
 327 however, the larger spatial scale outperforms the smaller spatial scale, which completely loses track
 328 of the climate change.

4 DISCUSSION

329 Animals navigate complex, dynamic and patchy environments. When there is a strongly localized
 330 and seasonal component to the resource dynamics, movement strategies limited to straightforward
 331 resource-following taxis necessarily fail to maximally exploit available resources. It is in these cases,
 332 quite common in the natural world, that seasonal migration becomes a viable, even necessary,

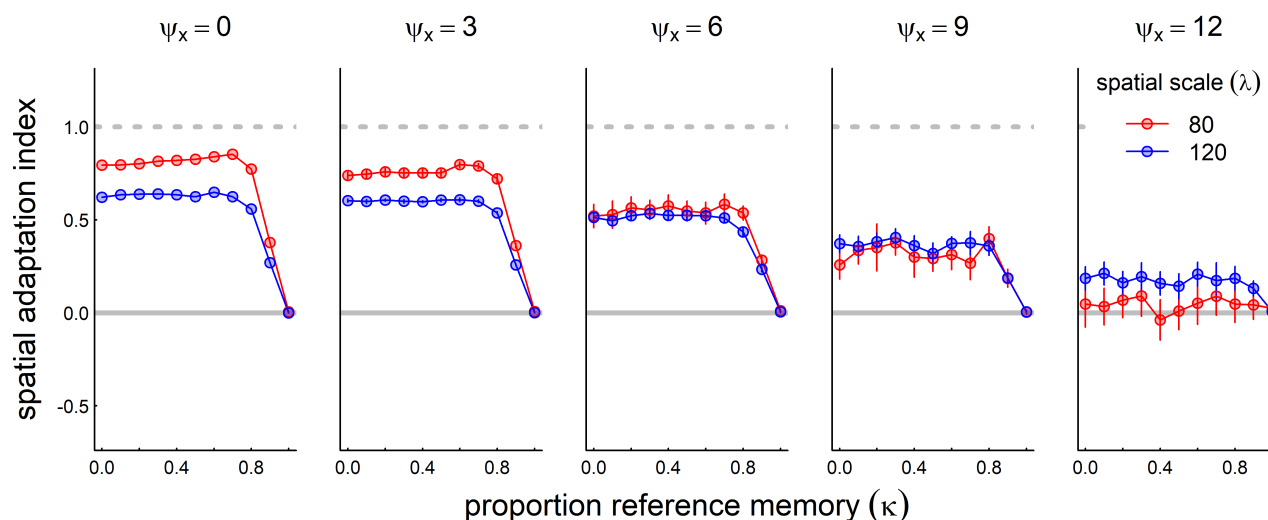


Figure 8. Role of reference memory in adapting to climate change for increasingly stochastic resource dynamics. We ran the model with a moderate rate of climate change (mean shift: 0.5/year) at five increasing levels of stochasticity (inter-annual standard deviation of resource peak 0, 3, 6 and 12, left to right panels). For non-zero stochasticity, we ran the process 30 times and present the mean and standard error of the spatial adaptation index across various values of the reference memory parameter κ : where $\kappa = 0$, the system modifies its migration based entirely on recent experiences; at $\kappa = 1$, the memory never changes from the reference memory. Other parameter values are resource following $\alpha = 100$, social attraction $\beta = 400$, and diffusion $\varepsilon = 4$.

strategy. However, when resources start shifting in space and time – as is occurring at an accelerated pace with recent global climate change – the migration phenology itself must exhibit some plasticity. It is our conjecture that this plasticity is facilitated by a memory-driven process in which recent experiences inform strategic behaviors in subsequent years. The relatively simple, social and memory-driven mechanism we propose here was, in fact, able to adapt to long-term changes in resource dynamics, even with inter-annual stochasticity. The model thereby provides a framework with which the interaction of memory, movement, social and resource dynamics can be further explored.

4.1 Adaptation and resiliency

By allowing a population to adjust its migratory behavior based on recent experiences with the resource location, our model captured many fundamental phenomena related to migration. The model was able to emulate the successful navigation of an environment with temporally and spatially isolated seasonal resource patches, the emergence of a migratory behavior from an essentially resident or naive initial condition, and intrinsic robustness to changes in those environmental resources, whether those changes were steadily shifting trends or inter-annual stochasticity. In a generalized way, it captured all three fundamental types of migration plasticity: the *where*, the *when* and the *whether* (Xu et al., 2021).

Our goal was to understand the combinations of factors that lead to a resilient migration behavior. We used foraging efficiency as a convenient metric of the utility of migration, though this was not a measure explicitly maximized by the model. Other metrics, such as foraging efficiency in a given season, or probability of survival or reproduction relative to resource availability (Bauer et al., 2020) may respond differently across model parameters and could be useful in understanding the relative success of alternative migratory strategies in different contexts. However, the overall annually

355 averaged metric provided the broadest linkage between resource dynamics and animals' locations
356 and was consistent with the minimal biological assumptions and generality of our framework.

357 Sociality parameters – in particular, the spatial scale λ – were, unexpectedly among the most
358 important parameters for determining the resiliency of the process. Populations with small spatial
359 scales tended to have a more difficult time locking in to an adaptive migratory pattern, and only when
360 social attraction was relatively weak. On the other hand, overly large spatial scales compromised
361 the ability of the process to track climate change, due to a dilution of the population's ability to
362 concentrate over available resource patches and remember the corresponding benefits.

363 The ability to adapt a migration also depended strongly on properties of the resource dynamics.
364 In particular, the reinforcement of memory and foraging is strongest when patches are concentrated
365 in time, but relatively large in space. Interestingly, in most stable patterns, the eventual targeted
366 migration arrival time coincided with the *peak*, rather than the beginning, of the resource dynamic.
367 This indicates that the long-distance social migration behavior may be particularly reinforced when
368 the targeted resource is very sudden. This is the case for the rapid green-up that occurs in high
369 latitudes as snow recedes in tandem with extended day lengths leading to an intense green-up period
370 (Park et al., 2020) or, for example, when resources are linked to the short-duration early blooming
371 phenology of very particular plants (Post and Forchhammer, 2007; Renner and Zohner, 2018).

372 Even with no strong intrinsic propensity to migrate and a weak phenological resource pulse to
373 follow, our model captured the ability to acquire a strong and adaptive migration behavior (figure 5).
374 Learning migration, however, requires a very strong resource attraction, higher levels of exploratory
375 behavior (e.g. diffusion, and larger spatial scale of sociality), and – often — many more years,
376 findings that echo empirical observations (Jesmer et al., 2018).

377 Despite the ability of the process to adapt under many stable conditions, our migration model
378 (and, perhaps, migration behaviors in general) can also be considered somewhat fragile. Under
379 many shifting conditions, e.g. increasing stochasticity, rapidly shifting resources, a shift in some of
380 the system parameters, or even a shift in the spatial and temporal extent of resources, migration
381 can collapse and turn into a non-migratory, residential behavior (figure 3). This sensitivity may
382 explain why partially migratory populations are so common and, apparently, evolutionary stable
383 (Berthold, 1999; Chapman et al., 2011), as well as the wide range of migration plasticity shown in
384 wild populations, even within a species (Xu et al., 2021).

385 4.2 Biological interpretation of parameters

386 All of the parameters in our model have well-defined biological interpretations. The diffusion
387 (ε) captures short time-scaled randomness of movement, reflecting exploratory and short-term
388 dispersive behavior. The foraging advection strength (α) captures the attraction of the population
389 to better quality resources at a relatively large scale. These two parameters, the basic ingredients
390 in diffusion-advection models of animal movement, have direct parallels to empirically estimated
391 properties of animal behavior: diffusion is closely related to families of random walk models (Gurarie
392 and Ovaskainen, 2011) while the advective taxis is related to the step- and resource selection
393 functions that are routinely estimated from movement data (Potts and Schlägel, 2020). The spatial
394 scale of the social group (λ) captures the spatial extent of the population, i.e. a population-level
395 home range (Noonan et al., 2019). We note, however, that diffusion-advection models can also be
396 interpreted as a probabilistic description of a single individual's movement. In this case, λ would
397 correspond to an individual home-range and β would be an individual's tendency to be drawn to

the center of that home range, akin to an individual migratory Ornstein-Uhlenbeck process (Gurarie et al., 2017).

The sociality parameter (β) quantifies the strength an individual's desire to approach the center of the social group. While this parameter is not typically measured, it may in principle be possible to estimate in a manner analogous to step-selection function by replacing environmental variables with presence of conspecifics as a covariate. The ratio between α and β can be interpreted as the relative importance of foraging to social cohesion, which appears to be important in predicting the resilience of migration.

Migration timing and location parameter can be straightforwardly estimated from movement data (Cagnacci et al., 2015; Gurarie et al., 2019) and synchrony of migration timing and site fidelity are well-documented for many migratory species (Joly et al., 2021). Thus, for example, Gurarie et al. (2019) explicitly estimated the ranging area, timing, and seasonal range locations for migratory caribou, identifying the kind of inter-annual variation that is reflected in the stochastic scenarios explored here as well as trends in timing.

The reference memory parameter κ is, of course, impossible to observe directly. Our model does, however, allow us to explore in an heuristic way the conditions under which a strong cultural tendency to migrate with certain fixed patterns can help a population hedge against stochasticity (Abrahms et al., 2019; Fagan, 2019). An extremely conservative behavior is the best way to hedge against stochasticity with no directional changes (high κ values in figure 7), as there is no benefit to change behavior based on recent experiences if they provide no information about future conditions. However, this extreme conservatism is, by definition, incapable of adapting when there is a consistent shift in resource distribution (figure 8). In cases where both processes are occurring, we did see a slight improvement in adaptability when long-term reference memory was balanced against a strong response to recent experience (see peaks in 8).

We'll note that our exploration of the model was not exhaustive. We did not explore, for example, the resilience of the migration process to changes in phenology timing. We hope that making the model available, including via an interactive interface, will facilitate those explorations.

4.3 Social learning and collective knowledge

Models have shown that collective knowledge is important, if not essential, to the evolution and process of migration (Shaw and Couzin, 2013; Guttal and Couzin, 2010; Berdahl et al., 2018). Many migratory organisms are social, and social learning is an acknowledged, non-genetic method for transmitting information (Kashetsky et al., 2021). Because our model is not individual-based, we can not identify any specific mechanism (e.g. leader-follower) of social information transfer. But, in a generic way, our model assumes that migration is driven by a collective trigger for the timing and locations of seasonal ranges, which is consistent with the known social and exogenous (e.g. daylength related) triggers for migration. Further, the underlying assumption of the migration "urge" is consistent with the strong endogenous programs to migrate, e.g. the seasonal restlessness known as *Zugunruhe* exhibited by many birds (Berthold, 1999; Helm, 2006).

In contrast to the many individual-based models of the evolution of migration (e.g. Guttal and Couzin, 2010; Shaw and Couzin, 2013; Anderson et al., 2013), our model did not include any selection, inheritance or birth or death processes. For example, Anderson et al. (2013) explored the resilience of a population under selective pressure under persistent trends and increased stochasticity of a drifting optimal resource window, showing that a certain amount of heritable phenotypic

441 plasticity is necessary to adapt successfully to climate change even at the cost of efficiency. Our
442 model underscores the fact that some level of resilience and adaptability can be attained with
443 a purely cognitive process that balances sociality with long and short term collective memory.
444 Importantly, this knowledge can be transmitted through social and cultural, rather than genetic,
445 pathways. The high level of sociality among migratory animals, as well as multi-annual parent
446 offspring bonds, are an evident pathway for that kind of transmission. As with those evolutionary
447 models, however, it is clear that when changes are too rapid, no amount of cognition can help
448 entirely mitigate against adverse outcomes. Furthermore, if behaviors are not sufficiently plastic
449 (i.e., if κ is too close to 1), then adaptation is very difficult.

450 Given the slow scale of fitness selection and the constant change in environmental conditions, it is
451 possible that certain inherent properties of populations, for example the “conservatism” captured
452 by the κ parameter, are themselves selected for to maximize resilience over a long time scale in
453 stochastic environments.

454 **4.4 Summary**

455 Rapid environmental change, both global warming and increased anthropogenic development, is
456 causing severe and dramatic impacts to the widespread and generally successful strategy of seasonal
457 migration for many taxa, and the fate of many animal migrations is a topic of increasing concern
458 (Wilcove and Wikelski, 2008; Kauffman et al., 2021). The ability of animals to respond to these
459 changes depends deeply on their behavioral plasticity and cognitive abilities. The importance of those
460 abilities is in direct proportion to the difficulty in studying them directly. By quantitatively exploring
461 the properties of a heuristic model that distill many of the main properties of wild populations in
462 dynamic and seasonal environments, we hope to have identified some broad patterns that might
463 guide further empirical exploration of the cognitive underpinnings of adaptability and resilience.

CONFLICT OF INTEREST STATEMENT

464 The authors declare that the research was conducted in the absence of any commercial or financial
465 relationships that could be construed as a potential conflict of interest.

AUTHOR CONTRIBUTIONS

466 EG and WFF provided the original idea. EG and SP developed and ran models and analysis. All
467 authors contributed to the writing.

FUNDING

468 EG, WFF, GCC and RSC, were supported in part by NSF award DMS 1853478. EG and WFF
469 were further partially supported by NSF grant IIBR 1915347.

ACKNOWLEDGMENTS

470 The authors are grateful to Quentin Read at SESYNC for computational support and advice for
471 multi-node multi-core model runs.

DATA AVAILABILITY STATEMENT

472 The only data analyzed in this manuscript was generated by simulation scripts made available in
473 the GitHub repository at <https://github.com/EliGurarie/memorymigration>.

REFERENCES

- Abrahms, B., Hazen, E. L., Aikens, E. O., Savoca, M. S., Goldbogen, J. A., Bograd, S. J., et al. (2019). Memory and resource tracking drive blue whale migrations. *Proceedings of the National Academy of Sciences* 116, 5582–5587.
- Anderson, J. J., Gurarie, E., Bracis, C., Burke, B. J., and Laidre, K. L. (2013). Modeling climate change impacts on phenology and population dynamics of migratory marine species. *Ecological Modelling* 264, 83–97.
- Avgar, T., Street, G., and Fryxell, J. M. (2014). On the adaptive benefits of mammal migration. *Canadian Journal of Zoology* 92, 481–490. doi:10.1139/cjz-2013-0076
- Bauer, S., McNamara, J. M., and Barta, Z. (2020). Environmental variability, reliability of information and the timing of migration. *Proceedings of the Royal Society B: Biological Sciences* 287, 20200622. doi:10.1098/rspb.2020.0622
- Berdahl, A. M., Kao, A. B., Flack, A., Westley, P. A., Codling, E. A., Couzin, I. D., et al. (2018). Collective animal navigation and migratory culture: from theoretical models to empirical evidence. *Philosophical Transactions of the Royal Society B: Biological Sciences* 373, 20170009. doi:10.1098/rstb.2017.0009
- Berthold, P. (1999). A comprehensive theory for the evolution, control and adaptability of avian migration. *Ostrich* 70, 1–11. doi:10.1080/00306525.1999.9639744
- Bhattacharyya, A. (1943). On a measure of divergence between two statistical populations defined by their probability distributions. *Bull. Calcutta Math. Soc.* 35, 99–109.
- Bischof, R., Loe, L. E., Meisingset, E. L., Zimmermann, B., Van Moorter, B., and Mysterud, A. (2012). A migratory northern ungulate in the pursuit of spring: jumping or surfing the green wave? *The American Naturalist* 180, 407–424.
- Bracis, C. and Mueller, T. (2017). Memory, not just perception, plays an important role in terrestrial mammalian migration. *Proceedings of the Royal Society B: Biological Sciences* 284, 20170449.
- Breiman, L. (2001). Random forests. *Machine learning* 45, 5–32.
- Cagnacci, F., Focardi, S., Ghisla, A., van Moorter, B., Merrill, E. H., Gurarie, E., et al. (2015). How many routes lead to migration? comparison of methods to assess and characterize migratory movements. *Journal of Animal Ecology* 85, 54–68. doi:10.1111/1365-2656.12449
- Chapman, B. B., Brönmark, C., Nilsson, J.-Å., and Hansson, L.-A. (2011). The ecology and evolution of partial migration. *Oikos* 120, 1764–1775. doi:10.1111/j.1600-0706.2011.20131.x
- Dingle, H. (2014). *Migration: the biology of life on the move* (Oxford University Press, USA).
- Elzhov, T. V., Mullen, K. M., Spiess, A.-N., and Bolker, B. (2016). *minpack.lm: R Interface to the Levenberg-Marquardt Nonlinear Least-Squares Algorithm Found in MINPACK, Plus Support for Bounds*. R package version 1.2-1.
- Fagan, W., Gurarie, E., Bewick, S., Howard, A., Cantrell, R., and Cosner, C. (2017). Perceptual ranges, information gathering, and foraging success in dynamic landscapes. *The American Naturalist* 189, 474–489. doi:10.1086/691099
- Fagan, W., Hoffman, T., Dahiya, D., Gurarie, E., Cantrell, R., and Cosner, C. (2019). Improved foraging by switching between diffusion and advection: benefits from movement that depends on spatial context. *Theoretical Ecology* 13, 127–136. doi:10.1007/s12080-019-00434-w
- Fagan, W. F. (2019). Migrating whales depend on memory to exploit reliable resources. *Proceedings of the National Academy of Sciences* 116, 5217–5219. doi:10.1073/pnas.1901803116
- Fagan, W. F., Cantrell, R. S., Cosner, C., Mueller, T., and Noble, A. E. (2011). Leadership, social learning, and the maintenance (or collapse) of migratory populations. *Theoretical Ecology* 5,

- 253–264. doi:10.1007/s12080-011-0124-2
- Festa-Bianchet, M., Ray, J., Boutin, S., Côté, S., and Gunn, A. (2011). Conservation of caribou (*Rangifer tarandus*) in Canada: an uncertain future. *Canadian Journal of Zoology* 89, 419–434. doi:10.1139/z11-025
- Fryxell, J. M., Greever, J., and Sinclair, A. (1988). Why are migratory ungulates so abundant? *The American Naturalist* 131, 781–798
- Gurarie, E., Cagnacci, F., Peters, W., Fleming, C. H., Calabrese, J. M., Mueller, T., et al. (2017). A framework for modelling range shifts and migrations: asking when, whither, whether and will it return. *Journal of Animal Ecology* 86, 943–959
- Gurarie, E., Hebblewhite, M., Joly, K., Kelly, A. P., Adamczewski, J., Davidson, S. C., et al. (2019). Tactical departures and strategic arrivals: Divergent effects of climate and weather on caribou spring migrations. *Ecosphere* 10, e02971
- Gurarie, E. and Ovaskainen, O. (2011). Characteristic spatial and temporal scales unify models of animal movement. *The American Naturalist* 178, 113–123
- Guttal, V. and Couzin, I. D. (2010). Social interactions, information use, and the evolution of collective migration. *Proceedings of the National Academy of Sciences* 107, 16172–16177. doi:10.1073/pnas.1006874107
- Hardesty-Moore, M., Deinet, S., Freeman, R., Titcomb, G. C., Dillon, E. M., Stears, K., et al. (2018). Migration in the anthropocene: how collective navigation, environmental system and taxonomy shape the vulnerability of migratory species. *Philosophical Transactions of the Royal Society B: Biological Sciences* 373, 20170017. doi:10.1098/rstb.2017.0017
- Helm, B. (2006). Zugunruhe of migratory and non-migratory birds in a circannual context. *Journal of Avian Biology* 37, 533–540. doi:10.1111/j.2006.0908-8857.03947.x
- Jesmer, B. R., Merkle, J. A., Goheen, J. R., Aikens, E. O., Beck, J. L., Courtemanch, A. B., et al. (2018). Is ungulate migration culturally transmitted? Evidence of social learning from translocated animals. *Science* 361, 1023–1025
- Joly, K., Gurarie, E., Hansen, D. A., and Cameron, M. D. (2021). Seasonal patterns of spatial fidelity and temporal consistency in the distribution and movements of a migratory ungulate. *Ecology and Evolution* 11, 8183–8200. doi:10.1002/ece3.7650
- Kashetsky, T., Dukas, R., and Avgar, T. (2021). The cognitive ecology of animal movement. *Frontiers in Ecology and Evolution (this issue)*
- Kauffman, M. J., Cagnacci, F., Chamaillé-Jammes, S., Hebblewhite, M., Hopcraft, J. G. C., Merkle, J. A., et al. (2021). Mapping out a future for ungulate migrations. *Science* 372, 566–569. doi:10.1126/science.abf0998
- Kölzsch, A., Bauer, S., De Boer, R., Griffin, L., Cabot, D., Exo, K.-M., et al. (2015). Forecasting spring from afar? Timing of migration and predictability of phenology along different migration routes of an avian herbivore. *Journal of Animal Ecology* 84, 272–283
- Lin, H.-Y., Fagan, W. F., and Jabin, P.-E. (2021). Memory-driven movement model for periodic migrations. *Journal of Theoretical Biology* 508, 110486. doi:10.1016/j.jtbi.2020.110486
- Merkle, J. A., Monteith, K. L., Aikens, E. O., Hayes, M. M., Hersey, K. R., Middleton, A. D., et al. (2016). Large herbivores surf waves of green-up during spring. *Proceedings of the Royal Society B: Biological Sciences* 283, 20160456. doi:10.1098/rspb.2016.0456
- Merkle, J. A., Sawyer, H., Monteith, K. L., Dwinnell, S. P. H., Fralick, G. L., and Kauffman, M. J. (2019). Spatial memory shapes migration and its benefits: evidence from a large herbivore. *Ecology Letters* 22, 1797–1805. doi:10.1111/ele.13362

- Mogilner, A. and Edelstein-Keshet, L. (1999). A non-local model for a swarm. *Journal of Mathematical Biology* 38, 534–570. doi:10.1007/s002850050158
- Moore, S. E. and Huntington, H. P. (2008). Arctic marine mammals and climate change: Impacts and resilience. *Ecological Applications* 18, S157–S165. doi:10.1890/06-0571.1
- Noonan, M. J., Tucker, M. A., Fleming, C. H., Akre, T. S., Alberts, S. C., Ali, A. H., et al. (2019). A comprehensive analysis of autocorrelation and bias in home range estimation. *Ecological Monographs* 89, e01344
- Park, H., Jeong, S., and Peñuelas, J. (2020). Accelerated rate of vegetation green-up related to warming at northern high latitudes. *Global Change Biology* 26, 6190–6202. doi:10.1111/gcb.15322
- Post, E. and Forchhammer, M. C. (2007). Climate change reduces reproductive success of an arctic herbivore through trophic mismatch. *Philosophical Transactions of the Royal Society B: Biological Sciences* 363, 2367–2373. doi:10.1098/rstb.2007.2207
- Potts, J. R. and Schlägel, U. E. (2020). Parametrizing diffusion-taxis equations from animal movement trajectories using step selection analysis. *Methods in Ecology and Evolution* 11, 1092–1105. doi:10.1111/2041-210X.13406
- Renner, S. S. and Zohner, C. M. (2018). Climate change and phenological mismatch in trophic interactions among plants, insects, and vertebrates. *Annual Review of Ecology, Evolution, and Systematics* 49, 165–182. doi:10.1146/annurev-ecolsys-110617-062535
- Riotte-Lambert, L. and Matthiopoulos, J. (2020). Environmental predictability as a cause and consequence of animal movement. *Trends in Ecology & Evolution* 35, 163–174. doi:10.1016/j.tree.2019.09.009
- Robinson, R., Crick, H., Learmonth, J., Maclean, I., Thomas, C., Bairlein, F., et al. (2009). Travelling through a warming world: climate change and migratory species. *Endangered Species Research* 7, 87–99. doi:10.3354/esr00095
- Seebacher, F. and Post, E. (2015). Climate change impacts on animal migration. *Climate Change Responses* 2. doi:10.1186/s40665-015-0013-9
- Shaw, A. K. (2016). Drivers of animal migration and implications in changing environments. *Evolutionary Ecology* 30, 991–1007. doi:10.1007/s10682-016-9860-5
- Shaw, A. K. and Couzin, I. D. (2013). Migration or residency? the evolution of movement behavior and information usage in seasonal environments. *The American Naturalist* 181, 114–124
- Soetaert, K. and Meysman, F. (2012). Reactive transport in aquatic ecosystems: Rapid model prototyping in the open source software r. *Environmental Modelling and Software* 32, 49–60
- Soetaert, K., Petzoldt, T., and Setzer, R. W. (2010). Solving differential equations in R: Package deSolve. *Journal of Statistical Software* 33, 1–25. doi:10.18637/jss.v033.i09
- Uboni, A., Horstkotte, T., Kaarlejärvi, E., Sévêque, A., Stammler, F., Olofsson, J., et al. (2016). Long-term trends and role of climate in the population dynamics of eurasian reindeer. *PLoS ONE* 11, e0158359. doi:10.1371/journal.pone.0158359
- Wilcove, D. S. and Wikelski, M. (2008). Going, going, gone: Is animal migration disappearing. *PLoS Biology* 6, e188. doi:10.1371/journal.pbio.0060188
- Xu, W., Barker, K., Shawler, A., Scoyoc, A. V., Smith, J. A., Mueller, T., et al. (2021). The plasticity of ungulate migration in a changing world. *Ecology* 102. doi:10.1002/ecy.3293

1 SUPPLEMENTARY MATERIAL

1.1 Drifting resource

The drifting resource function has the following properties

1. The total amount of resource across space is constant throughout the year.
2. At the beginning, middle, and end of the year the resource is uniformly distributed.
3. At some peak time $\mu_t < \tau/2$, the resource concentrates at a location $\mu_x < \chi$ with a spatial deviation σ_x and a temporal deviation σ_t (where τ is the length of the year and χ is the extent of the spatial domain).
4. The resource peaks exactly symmetrically at time $\tau - \mu_t$ and location $-\mu_x$ with the same variances.

To generate a resource with these properties, we distributing the resource in space as a beta distribution, where the two shape and scale parameters vary sinusoidally in such a way as to fulfill the criteria above. Thus:

$$h(x, t, \theta) = \chi B(x/\chi, a(t, \theta), b(t, \theta))$$

where χ is the maximum value (domain) of x , $B(x, a, b)$ is the beta distribution, θ represents the set of parameters $t_r, x_r, \sigma_t, \sigma_x$, and the two shape parameters are given by:

$$a(t) = \frac{m}{s^2}(s^2 + m - m^2)$$

$$b(t, x', \sigma') = (m - 1) \left(1 + \frac{m}{s}(m - 1) \right)$$

where $m(t)$ and $s(t)$ describe the dynamic mean and variance of the resource peak. These equations are solutions to the mean and variance of the beta distribution, $\mu = \alpha/(\alpha + \beta)$, $\sigma^2 = \frac{\alpha\beta}{(\alpha+\beta)^2(\alpha+\beta+1)}$.

The means and variances themselves are Gaussian pulses, with the mean peaking at μ_x at time μ_t with standard deviation σ_t and at $-\mu_x$ at time $\tau - \mu_t$ and the standard deviation pulsing from $2\chi/\sqrt{12}$ (corresponding to a uniform distribution over the domain $-\chi$ to χ) at times 0, $\tau/2$ and τ down to σ_x at t_r and $\tau - t_r$, with standard deviation (in time) σ_t .